

TOMOSAR AND PS-INSAR ANALYSIS OF HIGH-RISE BUILDINGS IN BERLIN

Timo Balz¹, Lianhuan Wei¹, Michael Jendryke¹, Daniele Perissin², Mingsheng Liao¹

¹State Key Laboratory of Information Engineering in Surveying, Mapping and Remote Sensing, Wuhan University, Wuhan, China; balz@whu.edu.cn;

²Institute of Space and Earth Information, Chinese University of Hong Kong, Hong Kong; daniele.perissin@cuhk.edu.hk

ABSTRACT

Using high-resolution SAR data stacks, a large amount of persistent scatterers (PS) can be found in urban areas, which are used for very detailed surface deformation monitoring. However, in dense urban areas, many of these points consist of more than one dominant scatterer in elevation direction. Using tomographic SAR, points with more than one scatterer are detected.

Index Terms— SAR, urban, PS-InSAR, TomSAR

1. INTRODUCTION

Using synthetic aperture radar (SAR), ground surface deformations can be measured with differential SAR interferometry (D-InSAR) or, if a large data stack is available, with Permanent Scatterer Interferometry (PS-InSAR), developed at Politecnico di Milano [1][2].

PS-InSAR can reduce temporal and geometric decorrelation by working on Permanent Scatterers (PS) that can be identified from long time series of interferometric SAR images. The different interferometric phase contributions of each PS are distinguished by a space-time analysis. PS-InSAR provides a much higher point density than the leveling benchmarks, allowing for a more dense subsidence mapping.

SAR tomography (TomoSAR) retrieves the distribution of scatterers in the elevation direction and the corresponding reflectivity. In this way, TomoSAR aims at real and unambiguous 3D SAR imaging, *i.e.* imaging also in the third coordinate: elevation [3]. While in SAR tomography an estimate of the scatterer density in elevation is derived, PS-InSAR tries to retrieve the coordinates of single points. Like PS-InSAR, TomoSAR uses SAR data stacks to establish a synthetic aperture in the elevation direction. It is the strictest way for 3D SAR imaging. The concept of 4-D SAR imaging (D-TomoSAR) was first applied to ERS data [4]. With high-resolution D-TomoSAR, the seasonal amplitude of buildings can be estimated [5].

In the following section, we are going to describe PS-InSAR and TomoSAR briefly. In section 3, PS-InSAR and

TomoSAR results in Berlin, derived from a stack of TerraSAR-X images are shown and discussed. Finally, conclusions are drawn.

2. PS-INSAR AND TOMOSAR

2.1 The PS-InSAR technique

PS-InSAR uses a series of (normally) more than 20 SAR images of the same area. This large amount of images is required to remove the atmospheric influences on the measurement by assuming that deformations are correlated in time but less correlated in space, whereas atmospheric influences are correlated in space but uncorrelated in time.

PS-InSAR works on the so-called persistent scatterers (PS), which are pixels that are coherent over a long time. PSs are mostly formed at manmade objects, typically at corners. Because a large amount of PS can be found in urban areas, PS-InSAR is especially applicable in urban areas.

For each PS, the wrapped phases in the differential interferograms can be decomposed into:

- the uncompensated topography,
- the motion of the target between the acquisitions,
- the object scattering phase related to the path length traveled in the resolution cell,
- the atmospheric phase accounting for signal delays,
- the phase caused by imprecise orbit data,
- and additive noise.

Finally, the phases are unwrapped and the unwrapped phases are divided into DEM error phase, deformation phase, atmospheric phase screen (APS) distribution of master and slave images and noise.

2.2 Tomographic SAR

Figure 1 shows the basic geometry of TomoSAR. Similar to PS-InSAR, TomoSAR uses a data stack of several acquisitions from slightly different viewing angles to reconstruct the reflectivity function along the elevation direction, which is ignored in PS-InSAR.

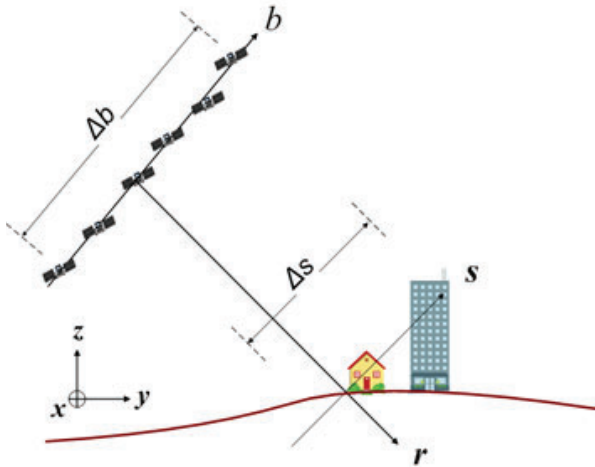


Figure 1. The TomoSAR principle

A focused SAR image could be considered as a projection of the 3D reflectivity scenario on azimuth-slant range plain. The combination of several acquisitions is used to form the so-called elevation aperture. Using spectral analysis for every azimuth-range pixel, a focused 3-D SAR image is obtained [6]. The objective of TomoSAR is to retrieve the reflectivity profile for each azimuth-range pixel and use it to estimate scattering parameters such as the number of scatterers present in the cell, their elevations, reflectivity, as well as their line-of-sight (LOS) deformation velocities in case of differential TomoSAR.

3. EXPERIMENTS IN BERLIN



Figure 2. Mean amplitude of the 25 spotlight images from Berlin (© DLR 2008/2009).

For our experiments we use a stack of 25 TerraSAR-X spotlight images acquired from 2008-2009. The mean amplitude image of the stack can be seen in Figure 2. In Figure 3, the temporal and spatial baselines of the SAR image stack are shown.

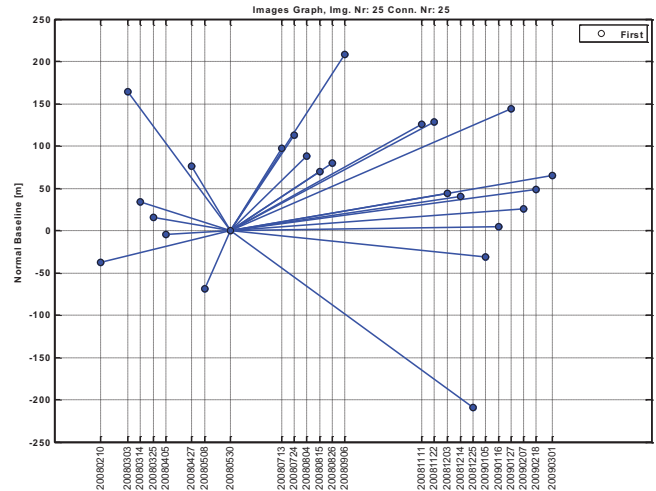


Figure 3. Temporal and spatial baselines of the stack

As test building we selected the Debis Tower in Berlin. The Debis Tower is a high-rise building, with an overall height of 106 meters on top of the tower. The main building part is a 23-floor office building, 85 meters high and each floor is approximately 3.7 meters high.

3.1 PS-InSAR analysis

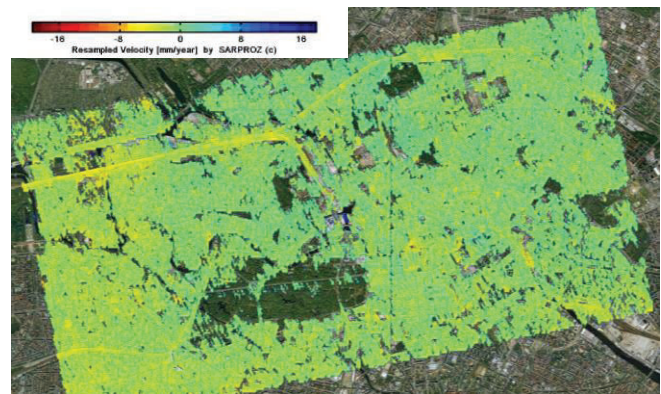


Figure 4. Deformation velocity estimation over Berlin.

The surface motion in the line-of-sight direction is estimated using a standard PS-InSAR approach with SARProZ [7]. From the overview in Figure 4, we can see that the area is quite stable during the measurement period.

Figure 5 shows the estimated deformation at the Debis Tower in Berlin. The PSs at the top of the tower are showing a rather strong subsidence. This is an error caused either by the seasonal deformation of the Debis Tower or by double scatterers at the upper building parts.



Figure 5. Deformation at the Debris-Tower, visualized using Google Earth

The PS points on the top of the tower and several points on the facade of the Debris Tower have a comparably low temporal coherence between 0.8-0.9, as shown in Figure 6. Compared to the very high coherences (> 0.9) achievable in other image parts, this is a relatively low coherence.



Figure 6. Temporal coherence of the PS points, visualized using Google Earth



Figure 7. Deformation after filtering at the Debris-tower, visualized using Google Earth

After filtering the comparably incoherent PS points, we can see in Figure 7, that there is no large deformation at or near the Debris Tower. One possible explanation for the rather low coherence is multiple scatterers occurring in one resolution cell. With tomographic techniques, we can estimate the number of scatterers per resolution cell in the test area.

3.2 Double-scattering detection

In SAR images of urban areas, we frequently find multiple scatterers in one resolution cell. Using tomographic techniques, points with one dominant scatterer and points with two or more dominant scatterers separated in elevation direction can be distinguished. Figure 8 shows the analysis of the scatterers on the Debris Tower.

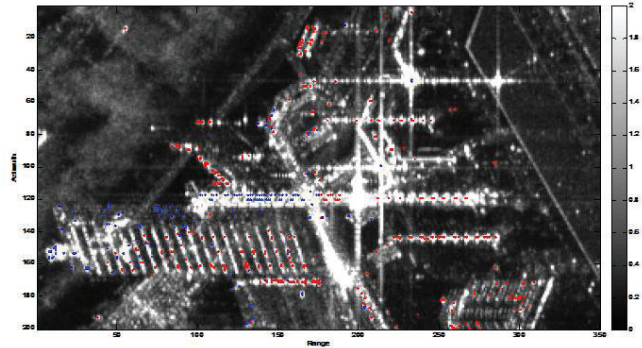


Figure 8. Distinguishing single- (red) and double-scattering (blue) points using TomoSAR on a stack of high-resolution spotlight TerraSAR-X images of Berlin. (TerraSAR-X data © DLR 2011)

We selected 529 points based on amplitude dispersion. The reflectivity profile of each point is reconstructed by a Truncated Singular Value Decomposition (TSVD) and a model selection to detect the number of scatterers and their position in elevation direction.

As shown in Figure 8, most of the single scatterers are at lower parts of buildings, while most double scatterers are at higher parts of buildings. This might be caused by the rather low resolution of TomoSAR in the elevation direction and might be different when using super resolution techniques [8].

3.3 Height Reconstruction

The height reconstruction of PS points using PS-InSAR works pretty well for single scatterers, as shown above. For testing the height reconstruction with TomoSAR, we select a point at the eighth floor of Debris office building, which is detected as a single scatterer with an elevation of 59 meters (see Figure 9(a)). Regarding the incidence angle of 30° , the estimated height of this scatterer should be 29.5 meters. Considering an average floor height of approximately 3.7 meters, the eighth floor should be about 29.6 meters high.

Our second test point is an estimated double scatterer. The profile of this point in elevation is shown below in Figure 9(b). Although the profile is strongly affected by side-lobes, two peaks are detected by the model selection process, with one stronger peak at an elevation of 85 m and a weaker

peak at an elevation of 291 m. The height difference between the two peaks corresponds to the building height. The estimated elevation distance of 206 meters corresponds to a height difference of 103 meters between the scatterers, regarding the 30° incidence angle, which is very close to the true building height of 106 m at the top of the tower.

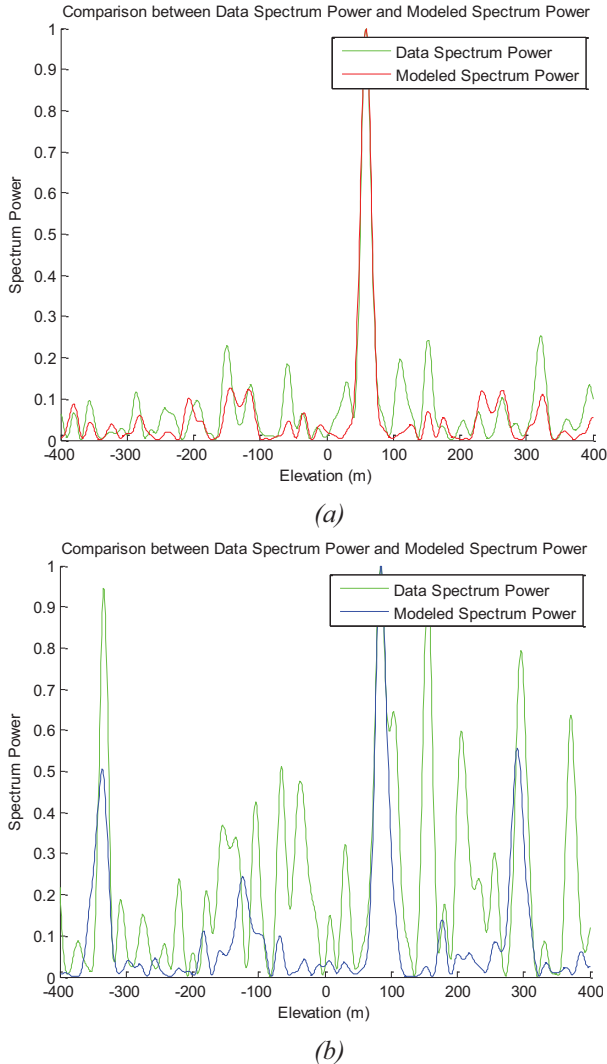


Figure 9. Example of a single scatterer (a) and a double scatterer (b) on the facade

4. CONCLUSIONS

PS-InSAR with high-resolution SAR data allows a precise measurement of surface motions. Typically, several PS points are found on a single building. Such a high PS density allows for an aggressive filtering of incoherent points.

Using tomographic techniques, PS points with multiple scatterers can be distinguished from single scatterer points. In dense urban environments, the number of PS points with multiple scattering centers is quite high. However, regarding

the high number of available PS points, it is useful to filter multi-scatterer points when applying PS-InSAR for surface motion surveillance. Alternatively, differential TomoSAR can be applied, when different surface motion velocities are expected at the different scatterers.

ACKNOWLEDGEMENT

The authors would like to thank the German Aerospace Center (DLR) for providing the test datasets via the DLR AO LAN0634. This work is financially supported by the National Natural Science Foundation of China (Grant No. 41174120), by the Research Fund for the Doctoral Program of Higher Education of China (Grant No. 20110141110057), by the National High Technology Research and Development Program of China (Grant No.2011AA120404), and by the International Graduate School of Science and Engineering, Technische Universität München, Munich.

REFERENCES

- [1] A. Ferretti, C. Prati, and F. Rocca, "Nonlinear subsidence rate estimation using permanent scatterers in differential SAR interferometry," *IEEE Transactions on Geoscience and Remote Sensing*, vol. 38, no. 5, pp. 2202-2212, 2000.
- [2] A. Ferretti, C. Prati, and F. Rocca, "Permanent scatterers in SAR interferometry," *IEEE Transactions on Geoscience and Remote Sensing*, vol. 39, no. 1, pp. 8-20, 2001.
- [3] A. Reigber and A. Moreira, "First demonstration of airborne SAR tomography using multibaseline L-band data," *IEEE Transactions on Geoscience and Remote Sensing*, vol. 38, no. 5, pp. 2142-2152, 2000.
- [4] G. Fornaro, D. Reale, and F. Serafino, "Four-Dimensional SAR Imaging for Height Estimation and Monitoring of Single and Double Scatterers," *IEEE Transactions on Geoscience and Remote Sensing*, vol. 47, no. 1, pp. 224-237, Jan. 2009.
- [5] X. Zhu and R. Bamler, "Let's Do the Time Warp: Multicomponent Nonlinear Motion Estimation in Differential SAR Tomography," *IEEE Geoscience and Remote Sensing Letters*, vol. 8, no. 4, pp. 735-739, 2011.
- [6] X. Zhu and R. Bamler, "Very High Resolution Spaceborne SAR Tomography in Urban Environment," *IEEE Transactions on Geoscience and Remote Sensing*, vol. 48, no. 12, pp. 4296-4308, 2010.
- [7] D. Perissin, Z. Wang, and T. Wang, "The SARPROZ InSAR tool for urban subsidence/manmade structure stability monitoring in China", in *Proc. ISRSE 2011*, Sidney, Australia.
- [8] X. Zhu and R. Bamler, "Super-Resolution Power and Robustness of Compressive Sensing for Spectral Estimation With Application to Spaceborne Tomographic SAR," *IEEE Transactions on Geoscience and Remote Sensing*, vol. 50, no. 1, pp. 247-258, 2011.